Methionine sulfoxide reductase 2 reversibly regulates Mge1, a cochaperone of mitochondrial Hsp70, during oxidative stress

Praveen Kumar Allu, Adinarayana Marada, Yerranna Boggula, Srinivasu Karri, Thanuja Krishnamoorthy, and Naresh Babu V. Sepuri
Department of Biochemistry, School of Life Sciences, University of Hyderabad, Gachibowli, Hyderabad 500046, India

ABSTRACT **Peptide methionine sulfoxide reductases are conserved enzymes that reduce oxidized methionines in protein(s). Although these reductases have been implicated in several human diseases, there is a dearth of information on the identity of their physiological substrates. By using *Saccharomyces cerevisiae* as a model, we show that of the two methionine sulfoxide reductases (MXR1, MXR2), deletion of mitochondrial MXR2 renders yeast cells more sensitive to oxidative stress than the cytosolic MXR1. Our earlier studies showed that Mge1, an evolutionarily conserved nucleotide exchange factor of Hsp70, acts as an oxidative sensor to regulate mitochondrial Hsp70. In the present study, we show that Mxr2 regulates Mge1 by selectively reducing MetO at position 155 and restores the activity of Mge1 both in vitro and in vivo. Mge1 M155L mutant rescues the slow-growth phenotype and aggregation of proteins of *mxr2*Δ strain during oxidative stress. By identifying the first mitochondrial substrate for Mxrs, we add a new paradigm to the regulation of the oxidative stress response pathway.**

Monitoring Editor
Thomas D. Fox
Cornell University

Received: Sep 13, 2014
Revised: Nov 17, 2014
Accepted: Nov 20, 2014

INTRODUCTION

Persistent oxidative stress is responsible for several neurological disorders, heart failure, and ageing (Finkel and Holbrook, 2000; Orrenius *et al.*, 2007). To combat oxidative stress, cellular systems have evolved several antioxidant defensive mechanisms. Methionine sulfoxide reductases (Msrs) are among the important regulators of oxidative stress (Levine *et al.*, 2000). These enzymes reduce either free or protein-bound oxidized methionine in a thioredoxin and thioredoxin reductase–dependent mechanism to prevent the accumulation of oxidized proteins and amino acids. In yeast, they are three methionine sulfoxide reductases, known as fRMsr, Mxr1/MsrA, and Mxr2/MsrB. The first is responsible for reducing free methionine sulfoxide (free Met-SO), and the last two are involved in the reduction of oxidized methionine present in proteins (Boschi-Muller *et al.*, 2008; Le *et al.*, 2009). Oxidation of methionine can produce a diastereomeric mixture of R and S methionine sulfoxide forms. Mxr1 apparently plays a role in reducing the S form of sulfoxide, whereas Mxr2 acts specifically on R sulfoxides. The mechanism of action of these enzymes has been well characterized in vitro using reconstitution assays containing purified Mxrs (Boschi-Muller *et al.*, 2008; Tarrago *et al.*, 2012). Homologues of Mxr proteins are present across evolution and have been found to play an essential role in the prevention of oxidative damage to proteins mediated by reactive oxygen species (ROS) in bacterial, plant, and animal cells (Zhang and Weissbach, 2008). These enzymes have been implicated in ageing and age-related disorders such as Alzheimer and Parkinson disease, cataract development, and insulin resistance (Gabbita *et al.*, 1999; Kantorow *et al.*, 2004; Glaser *et al.*, 2005; Styskal *et al.*, 2013). Despite their clinical relevance, there is a paucity of information on the identity of the physiological substrates of Mxrs and their regulation. Several reports suggest NF-κBα, potassium channel, and calmodulin as possible substrates of Mxrs (Ciorba *et al.*, 1997; Midwinter *et al.*, 2006; Erickson *et al.*, 2008). In a recent report, SelR, a homologue of MsrB in *Drosophila*, was shown to reduce the oxidized R form of methionine in actin and thereby regulate actin polymerization (Hung *et al.*, 2013). In mammals, MsrA has two isoforms present in mitochondria and cytosol, whereas MsrB has multiple isoforms

This article was published online ahead of print in MBoC in Press (http://www.molbiolcell.org/cgi/doi/10.1091/mbc.E14-09-1371) on November 26, 2014.

Address correspondence to: Naresh Babu V. Sepuri (nareshuohyd@gmail.com, nbvssl@uohyd.ernet.in).

Abbreviations used: Hsp70, heat shock protein 70; MALDI-TOF, matrix-assisted laser desorption/ionization time-of-flight; Mge1, mitochondrial GrpE; Mxr, methionine sulfoxide reductase; Tim23, translocase of inner membrane 23.

scattered in various organelles of the cell. Multiple forms of Msrs have also been detected in mammalian mitochondria (Kim and Gladyshev, 2004). In yeast, Mxr1 is localized to cytosol, whereas Mxr2 is present in mitochondria. In yeast, deletion of MXR1 or MXR2 or both abolishes growth on nonfermentable carbon sources, indicating that mitochondrial function is derailed (Kaya *et al.*, 2010). However, the precise role of Mxr1 or Mxr2 in mitochondria and their physiological substrates has yet to be discovered.

Mitochondrial biogenesis requires continuous translocation of nucleus-encoded and cytoplasm-synthesized proteins to different compartments of mitochondria (Chacinska *et al.*, 2009; Tammineni *et al.*, 2013). Oxidative conditions within the cell influence the import of preproteins into mitochondria (Wright *et al.*, 2001). Pretreatment of mitochondria with antimycin A, a superoxide-generating oxidizing agent, reduces the import of proteins into mitochondria in vitro. We recently discovered that a component of the mitochondrial protein import machinery, Mge1, acts as an oxidative sensor to regulate protein import into mitochondria and that this mechanism is likely to be conserved across evolution (Marada *et al.*, 2013).

Mge1 is an essential component of the molecular protein import motor present in the mitochondrial matrix. The other components of the molecular motor are Pam18, Pam16, and Hsp70 (Laloraya *et al.*, 1995; Grimshaw *et al.*, 2001). Proteins targeted to mitochondrial matrix require TOM and TIM complexes, which are present in the outer and inner membranes of mitochondria, respectively (Chacinska *et al.*, 2009). The incoming precursor protein emerging from the TIM complex interacts with Tim44 and Hsp70 in an ATP-dependent manner (D'Silva *et al.*, 2004). Hydrolysis of ATP on Hsp70 results in an Hsp70-ADP complex that has a high affinity for preproteins. Mge1, an adenine nucleotide exchange factor, in its active dimeric form exchanges ATP for ADP on Hsp70 and thereby facilitates the release of precursor protein from Hsp70 (Mayer and Bukau, 2005). In addition, Mge1 also plays a critical role in protein folding and in the biogenesis of iron–sulfur clusters (Westermann *et al.*, 1995; Lutz *et al.*, 2001).

In response to heat or oxidative stress, Mge1 monomerizes and fails to interact with Hsp70-ADP complex. This failure results in the halting of protein import into mitochondria. We recently showed that the lone methionine at position 155 in Mge1 is crucial for the oxidative sensor function of Mge1. A single point mutation of methionine to leucine at position 155 (M155L) within Mge1 prolongs the time taken for the cell to respond to oxidative stress (Marada *et al.*, 2013).

In this article, we present in vivo and in vitro evidence that Mge1, a conserved and an essential protein of mitochondria, is a physiological substrate of Mxr2. Using genetic and biochemical methods, we show that Met-155 in Mge1 gets oxidized, and the oxidized Mge1 interacts with Mxr2. Mxr2 specifically reduces the oxidized Met-155 in Mge1 both in vivo and in vitro. Of most importance, Mge1 M155L mutant rescues the protein aggregation and slow-growth phenotype of *mxr2*Δ during oxidative stress. Our studies reveal a novel reversible mechanism that the cell uses to regulate oxidative stress in mitochondria.

RESULTS

Deletion of MXR2 exacerbates sensitivity to H_2O_2

Yeast Mxr1 and Mxr2 are peptide methionine sulfoxide reductases located in the cytoplasm and mitochondria, respectively. Given the similar function for both enzymes, we investigated whether their functions are redundant in the oxidative stress response pathway. Oxidative stress response can be elicited in yeast cells by addition of H_2O_2. Hence we monitored the growth of serially diluted yeast *Saccharomyces cerevisiae* cells in wild type (BY4741), deleted for MXR1 (*mxr1*Δ), or deleted for MXR2 (*mxr2*Δ) on yeast extract/peptone/dextrose (YPD) plates with or without the addition of 1 mM H_2O_2. Both deletion strains exhibited normal growth, similar to wild-type strain on control YPD plates (Figure 1A, top left), whereas slow growth was observed in the case of all the strains on YPD plates with 1 mM H_2O_2. Of most interest, cells deleted for MXR2 were found to be highly sensitive to H_2O_2 compared to wild- type or *mxr1*Δ strains (Figure 1A, top right). Similar results were obtained when we grew all the strains in liquid YPD medium with or without H_2O_2 (Figure 1B). These results implicate Mxr2 rather than Mxr1 as having a potential role in the oxidative stress response pathway. However, yeast having a double deletion of MXR1 and MXR2 are much more sensitive to H_2O_2 than yeast harboring only the MXR2 deletion (Supplemental Figure S1).

Epifluorescence studies have shown that green fluorescent protein GFP–Mxr2 is present in the mitochondria, whereas GFP-Mxr1 stays in the cytoplasm (Kaya *et al.*, 2010). However, the precise subcompartmental localization of Mxr2 within the mitochondria is not known. To determine the localization of Mxr2 within the mitochondria, we monitored the import of in vitro ^{35}S-labeled Mxr2 along with cytoplasm-localized Mxr1 and a known mitochondrial matrix–localized protein, Su9-DHFR, into mitochondria. Our results show that Mxr1 is poorly bound to mitochondria, as it is found to be sensitive to externally added protease, confirming its cytosolic localization (Figure 1C, bottom). We find that both Mxr2 and Su9-DHFR are enriched in the mitochondrial matrix fraction. Like Su9-DHFR, Mxr2 appears to be effectively processed by a mitochondrial matrix–localized processing peptidase, and the processed mature protein band is protected from the externally added trypsin (Figure 1C). However, both imported proteins become accessible to trypsin when the membranes are solubilized with Triton X-100 before protease treatment (Figure 1C, lane 5), indicating the matrix localization of Mxr2 and Su9-DHFR. Valinomycin dissipates the membrane potential and inhibits the import of matrix-targeted proteins. We observe complete abolition of the import of Mxr2 into valinomycin-treated mitochondria (Figure 1C, lanes 3 and 4). To further confirm the matrix localization of Mxr2, we resolved the cytoplasmic and mitochondrial fractions from the strain expressing Flag-Mxr2 on SDS–PAGE before carrying out Western blot analysis using antibodies against proteins that are benchmarks for the two fractions, besides Flag antibody for detecting Mxr2. Flag-Mxr2 was detected only in the mitochondrial fraction (Figure 1D). Tom40, known to be enriched in the mitochondrial fraction, and Fun12, a marker for cytosolic fraction, were used as controls. The mitochondrial fraction was further subfractionated to mitoplasts or subjected to Triton X-100 treatment as described in *Materials and Methods*. The fractions containing mitochondria, mitoplasts, and Triton X-100 treated mitochondria were further incubated with or without Proteinase K and subjected to Western blot analysis. Proteins Tom40, CCP1, and aconitase, which are hallmarks of the outer membrane, inter membrane space, and matrix fractions, respectively, were used as controls. Flag-Mxr2 and aconitase were detected in the matrix fraction, as they were resistant to protease action in the mitochondria and mitoplasts fractions, whereas Tom40, and CCP1 protein were susceptible to protease treatment (Figure 1E). When the mitochondrial membranes were solubilized with Triton X-100, all proteins were susceptible to externally added protease (Figure 1E, lane 6). Taken together, these results clearly show that Mxr2 is targeted to matrix region of mitochondria and functions in the oxidative stress response pathway.

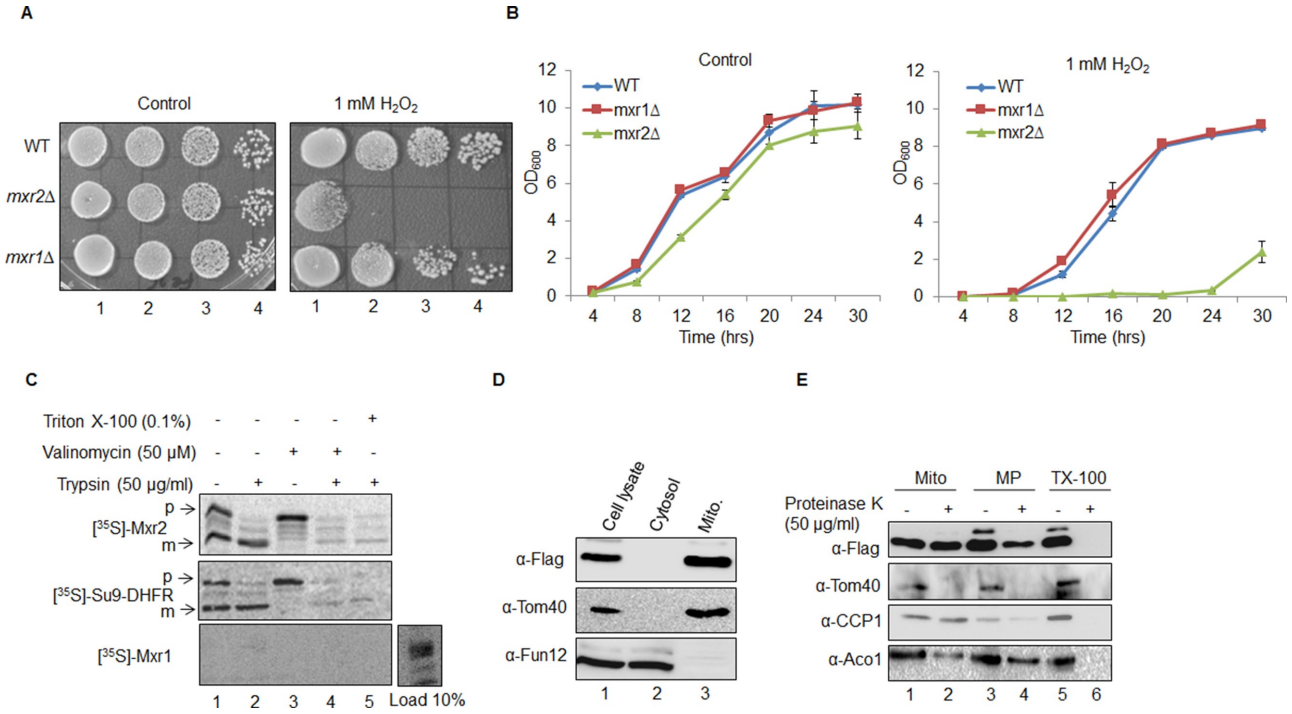

FIGURE 1: Mitochondrial localization and sensitivity of MXR2-deleted cells to H_2O_2. (A) Spotting assay. Yeast BY4741 (WT) strain and its derivatives *mxr1*Δ (yNB114) and *mxr2*Δ (yNB115) were tested for growth on solid and liquid medium and monitored for mitochondrial localization of proteins. All three strains were grown overnight in YPD medium. Cells at 0.5 OD were serially diluted (1:10), and 10 μl of each suspension was spotted on YPD plates supplemented with or without 1 mM H_2O_2 and incubated at 30°C for 2 d. (B) Strains were grown overnight in YPD medium before dilution in fresh YPD medium ± H_2O_2 (1 mM) and were allowed to grow at 30°C with shaking. Growth was monitored at various time points, as shown by taking the OD at 600 nm. (C) Autoradiogram of a mitochondrial import assay. ^{35}S-labeled Su9-DHFR, Mxr1, and Mxr2 proteins were incubated with mitochondria in the presence (lanes 3 and 4) or absence (lanes 1, 2, and 5) of 5 μM valinomycin. Import was carried out for 20 min at 30°C in the presence or absence of 50 μg/ml trypsin and Triton X-100 as shown. Samples were resolved on an SDS–PAGE gel and subjected to autoradiography. The "load" lane represents the 20% of Mxr1 that was used in the import assay. p, precursor; m, mature form of precursor protein. (D) Flag-Mxr2 protein localizes to mitochondria. Whole-cell extract (WCE; lane 1) of yeast strain expressing Flag-Mxr2 was subjected to differential centrifugation to fractionate mitochondrial (lane 3) and cytosolic fractions (lane 2). A Western blot probed with antibodies specific for Flag, Fun12, and Tom40. (E) Flag-Mxr2 is enriched in the mitochondrial matrix. Mitochondrial and mitoplast fractions were purified from a strain that expresses Flag-Mxr2. The two fractions were incubated with (lanes 2, 4 , and 6) or without proteinase K (lanes 1, 3, and 5). The mitochondrial fractions were additionally subjected to Triton X-100 (lanes 5 and 6). Samples were resolved by SDS–PAGE, Western transferred, and probed with antibodies that detect proteins that are hallmarks for various mitochondrial fractions—aconitase (mitochondrial matrix), CCP1 (intermembrane space), and Tom40 (outer membrane)—as well as Flag for finding submitochondrial localization of Mxr2.

Mxr2 interacts with Mge1 in an oxidative stress–dependent manner

We showed earlier that Mge1, a nucleotide exchange–stimulating factor of Hsp70, undergoes oxidation in the presence of H_2O_2 and thereby loses its stimulating activity. Like Mxr2, as shown here, Mge1 is also present in the mitochondrial matrix. Site-directed mutational studies suggested that Met-155, the lone methionine within Mge1, could be the likely oxidation site (Marada *et al.*, 2013). Given that both Mxr2 and Mge1 respond to H_2O_2-triggered oxidative stress and the complementing activity of Mxr2 for restoring the functions of methionine-oxidized proteins in vitro, we hypothesized that Mxr2 may be interacting with Mge1. To test our hypothesis, we initially expressed mature Mxr2 protein in its native form in bacterial cells. A prominent protein band corresponding to the molecular weight of Mxr2 (~15 kDa) is observed upon induction (Figure 2A, left). We previously described purification of recombinant His-Mge1 (Marada *et al.*, 2013), and Figure 2A, right, shows the purified product used in this study. Two equal amounts of recombinant purified His-Mge1 were taken and pretreated with or without H_2O_2 and mixed with soluble bacterial protein fraction enriched in native untagged Mxr2 and then allowed to bind to nickel-nitriloacetic acid (Ni-NTA) beads. After washing of the beads, Mge1 was eluted, resolved on SDS–PAGE, and stained with Coomassie blue. Mge1 was detected in the eluates from both beads (Figure 2B). However, a protein band corresponding to the molecular weight of Mxr2 was consistently observed only in the eluate from the beads that had H_2O_2-treated Mge1 (Figure 2B, lane 2). The band was excised from the gel and subjected to tandem mass spectrometry (MS/MS), and the protein was confirmed to be Mxr2 (Supplemental Figure S2). This finding suggests that Mxr2 has affinity only for Mge1, which is apparently oxidized by H_2O_2 in vitro.

Mxr2 harbors seven cysteine amino acids. The active site contains two Cys amino acids, known as catalytic cysteine and resolving cysteine, respectively (Tarrago *et al.*, 2012). The binding of Mxr2 to Mge1 may be mediated by cysteine amino acids present in Mxr2. To test the importance of cysteine amino acids in the binding

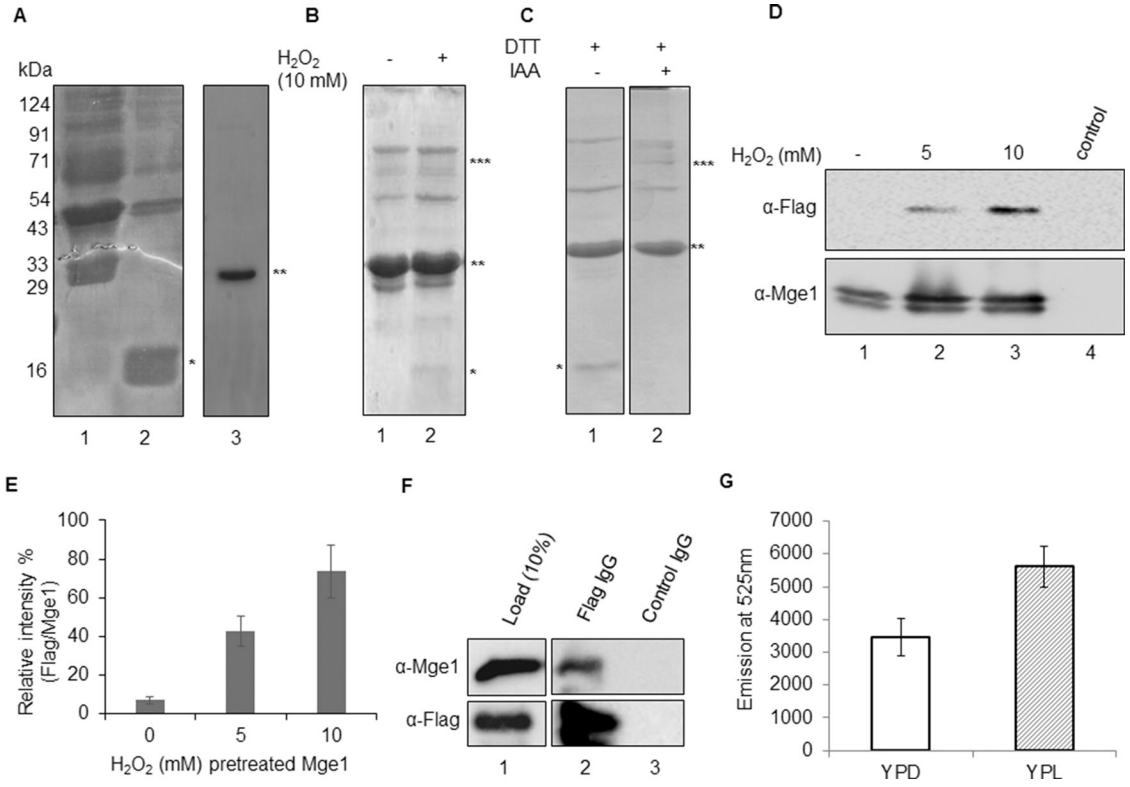

FIGURE 2: In vitro and in vivo interaction of Mxr2 with Mge1 in the presence of H_2O_2. (A) Soluble protein fractions were prepared from bacteria transformed with vector (lane 1) or vector expressing recombinant Mxr2 (lane 2). An aliquot of the soluble protein fractions was resolved by SDS–PAGE and the gel Coomassie stained (left). Purified recombinant His-Mge1 was resolved by SDS–PAGE, and the Coomassie stained gel is shown (right, lane 3). (B) Soluble protein fraction of bacterial transformant expressing Mxr2 was incubated with purified His-Mge1 that was pretreated with (lane 2) or without H_2O_2 (lane 1). His-Mge1 was recovered using Ni-NTA beads and resolved on SDS–PAGE, and the Coomassie-stained gel is shown. (*Mxr2, **Mge1-His, and ***nonspecific bands coeluted with Mge1). (C) Bacterial lysate expressing Mxr2 was treated with 10 mM DTT for 10 min before dividing it into two equal portions, with one portion treated with 50 mM IAA (lane 2). Both portions containing Mxr2 were incubated with purified His-Mge1 that was pretreated with H_2O_2. His-Mge1 and its interacting partners were recovered using Ni-NTA beads and separated on an SDS–PAGE, and the proteins resolved on the gel were stained with Coomassie. (D) Purified His-Mge1 was treated with increasing concentrations of H_2O_2 (lanes 2 and 3) and mixed with mitochondrial extracts prepared from yeast expressing Flag-Mxr2 as described in *Materials and Methods*. His-Mge1 and bound proteins were recovered using Ni-NTA beads. As a control (lane 4), Ni-NTA pull down was also performed using only mitochondrial extracts to exclude any nonspecific binding to the beads (lane 1). Samples were resolved on SDS–PAGE and subjected to immunoblot analysis for the presence of Flag-Mxr2 and Mge1. (E) Three independent blots of D were quantified to assess the relative quantity of Mge1 to Mxr2 using ImageJ software. (F) Immunoprecipitation of Flag-Mxr2. Flag-Mxr2 was immunoprecipitated from mitochondrial extracts prepared from yeast strain expressing Flag-Mxr2. A control immunoprecipitation was carried out using IgG (lane 3). Samples were resolved on SDS–PAGE and subjected to immunoblot analysis using antibodies specific for Flag and Mge1. (G) Yeast stains BY4741 were grown to early log phase in different media as shown, and ROS was measured as described in *Materials and Methods*. The histogram represents the average emission values of DCFDA at 525 nm from three replicates.

of Mxr2 to Mge1, we used the classical biochemical route of reducing the cysteine with dithiothreitol (DTT), followed by blocking it with iodoacetamide (IAA) to prevent reverse reaction. Bacterial lysate enriched for Mxr2 was initially treated with either DTT or DTT and IAA and then allowed to bind Ni-NTA beads prebound with H_2O_2-treated recombinant His-Mge1. The beads were washed, His-Mge1 was made to elute and resolved on SDS–PAGE, and the gel was stained with Coomassie (Figure 2C). A protein band corresponding to the molecular weight of Mxr2 is detected only in the eluate obtained from beads that had DTT-treated Mxr2. Recombinant H_2O_2-treated His-Mge1 was able to pull down Mxr2 from the bacterial lysate that was treated with DTT but failed to do so when DTT and IAA were added to the bacterial lysate (Figure 2C). These results show that cysteine residues within Mxr2 are important for efficient binding to Mge1. To test the specificity, we used recombinant H_2O_2-treated methionine substitution mutant (Mge1 M155L) in the pull- down assay and could not detect any Mxr2 in the eluate (Supplemental Figure S3). This finding suggests that Mxr2 has affinity only for Mge1 that is apparently oxidized by H_2O_2 in vitro. To extend these studies with isolated mitochondria, we repeated the binding assay, using cholate-solubilized mitochondrial extract prepared from yNB124 cells expressing Flag-Mxr2 as a source for Mxr2 instead of bacterial lysate and additionally pretreated recombinant His-Mge1 with increasing concentrations of H_2O_2. The eluates were resolved on SDS–PAGE, Western transferred, and probed with Mge1 and Flag antibodies. With increasing concentrations of H_2O_2, there is a concomitant increase in the binding of Flag-Mxr2, with the amount of Mge1 being almost same (Figure 2D). To

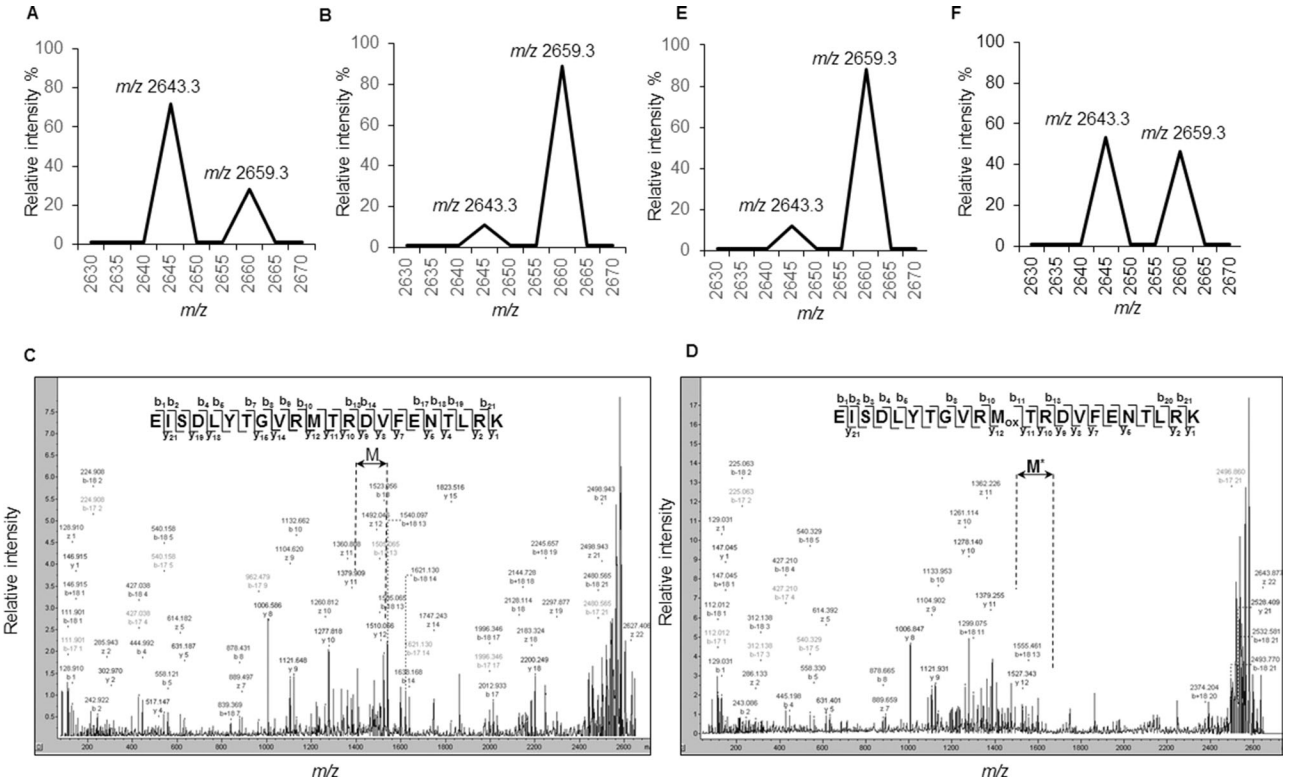

FIGURE 3: Met-155 in Mge1 is oxidized by H_2O_2 and reduced by Mxr2. (A, B) MALDI-TOF spectrum of Met-155 peptide from His-Mge1. Untreated His-Mge1 (A) and His-Mge1 treated with 20 mM H_2O_2 (B) were incubated at room temperature for 4 h and processed for MALDI-TOF as described in *Materials and Methods*. The peptides generated from LysC digestion were analyzed by a Bruker Daltonics mass spectrophotometer, and the MALDI-TOF spectrum of the Met-155–containing peptides is presented. (C). MS/MS spectrum of unoxidized (*m/z* 2643.3) peptide. (D). MS/MS spectrum of oxidized (*m/z* 2659.3) peptide. (E, F) Oxidized His-Mge1 was further treated with DTT (E) and DTT + Mxr2 (F) for 4 h before processing for MALDI-TOF. The MALDI-TOF spectrum of the Met-155 containing peptide is presented.

demonstrate that increased pull down of Flag-Mxr2 is indeed due to oxidation as opposed to better bait recovery, we quantified the amount of Mxr2 relative to that of Mge1 from three independent experiments and found that Flag-Mxr2 preferentially binds to oxidized Mge1 (Figure 2E).

On the basis of our in vitro and quasi–in vivo binding assays, we conclude that Mxr2 interacts with Mge1 in an oxidative stress dependent manner and that the cysteines within Mxr2 are crucial for this interaction. We next proposed to examine whether Mxr2 is indeed capable of interacting with Mge1 in the cellular context. Coimmunoprecipitation studies were carried out using mitochondria isolated from yeast cells expressing Flag-Mxr2. Mxr2 was immunoprecipitated with Flag antibody and probed with antibodies specific for Flag and Mge1 (Figure 2F). Intriguingly, Mge1 was detected in Flag-Mxr2 immunoprecipitates without the addition of any external oxidizing agent to the yeast cells grown in yeast extract/peptone/lactic acid (YPL) medium before isolation of mitochondria. We speculate that the internal ROS that is being produced in the mitochondrial milieu is sufficient to cause oxidation of at least a certain fraction of Mge1. To confirm our speculation, we measured the ROS levels in yeast cells grown in YPL medium and used cells grown in YPD as control. We observed relatively higher levels of ROS in yeast cells growing in YPL medium than in cells in YPD medium (Figure 2G). The cellular ROS level suggests that indeed it is possible that Mxr2 is interacting with Mge1 in an oxidation-dependent manner in vivo, a suggestion that is consistent with our in vitro findings.

Oxidation of Mge1 at methionine 155 and its subsequent reduction by Mxr2 in vitro

Amino acids like Cys, Met, Trp, Tyr, Phe, and His are most vulnerable to oxidation in a protein. Given that Mxr2 interacts with Mge1 in an oxidation-dependent manner, we investigated which amino acids within Mge1 are being targeted for oxidation. We used matrix-assisted laser desorption/ionization time-of-flight (MALDI-TOF) MS/MS analysis to evaluate peptide fragments generated from Mge1 as described in *Materials and Methods*. Purified recombinant His-Mge1 was pretreated with or without H_2O_2 before being resolved on an SDS–PAGE gel. Mge1 bands were in-gel digested with endoproteinase Lys-C and extracted peptides subjected to MALDI-TOF spectrum analysis. Peptides generated from Lys-C digestion (Supplemental Table S4) were monitored for their spectrum (Supplemental Figure S4). All the peptides had the expected MALDI-TOF *m/z* values except for the Met-155–containing peptide (Figure 3). This peptide from the untreated Mge1 protein displayed two *m/z* values—a relatively higher intensity peak of *m/z* value 2643.3 and a lower-intensity peak with *m/z* value of 2659.3 (Figure 3A). The difference in the *m/z* values of the two peaks obtained from the Met-155–containing peptide was ~16 Da. The Met-155–containing peptide from the oxidized Mge1 also displayed two peaks with ~16 Da difference in *m/z* values (Figure 3B). However, the second sample had a majority of the intensity coming from the peak that had *m/z* value of 2659.3 (Figure 3B). The intensity peak profile for the Met-155 peptide changed after oxidation (compare Figure 3, A and B).

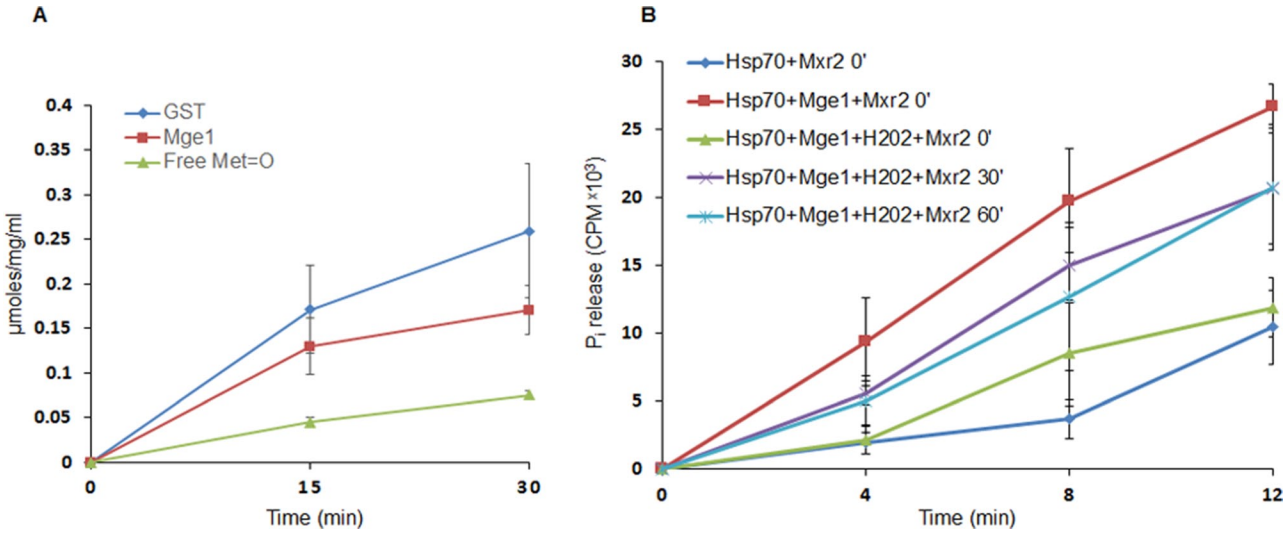

FIGURE 4: Mxr2 reduces oxidized Mge1 and restores ATPase activity of Mge1. (A) Purified recombinant His-Mge1 (50 µM) and GST (50 µM) proteins were treated with H_2O_2 before being used as substrates in Mxr2 enzymatic assay as described in *Materials and Methods*. Free methionine sulfoxide (Met-SO, 1 mM) was also included as a control substrate. Mxr2 activity was measured as a decrease in the absorption at $OD_{340\ nm}$. The graph represents the relative activity of the enzyme and is expressed as micromoles per milligram per milliliter. The basal activity observed in the absence of substrate was subtracted from the values obtained in the presence of substrate and enzyme. Given that there was no detectable enzymatic activity in the absence of Mxr2, this control is not shown. (B) Purified Mge1 was initially incubated with or without 5 mM H_2O_2 for 2 h in PBS, pH 7.2. Later, the proteins were treated with or without Mxr2 for 0, 30, or 60 min, followed by incubation with recombinant Hsp70 in an ATPase assay buffer as described previously (Marada *et al.*, 2013). The release of labeled P_i was monitored at different time points in a scintillation counter. A control Hsp70 sample was incubated with Mxr2 to monitor nonspecific ATP hydrolysis.

We further examined the Met-155–containing peptide from both the H_2O_2-untreated and -treated samples by MS/MS (Figure 3, C and D). From C-terminal sequencing, we find that all the amino acids were identical in both peptides up to methionine. In the case of the peptide from the oxidized sample, after Met, the subsequent peptide fragments show an apparent shift that corresponds to oxidation (Figure 3D). The difference between unoxidized and oxidized Met-155 of 16 Da was ascertained by comparing the y11 and y12 ions derived from C-terminal fragmentation. Addition of 16 Da indicates formation of methionine sulfoxide in the oxidized peptide. Formation of methionine sulfoxide was also confirmed by the presence of ions with loss of methane sulfenate (CH_3SOH, –64 Da) side chain due to instability of methionine sulfoxide immonium ion. MALDI-TOF MS/MS results provide evidence that Met-155 in Mge1 is oxidized in the presence of H_2O_2. They also show that the apparently unoxidized Mge1 is a mixture of a small fraction of oxidized and a major fraction of unoxidized Mge1.

Because the oxidized form of Mge1 alone is capable of significant interaction with Mxr2, we were interested to test whether Mxr2 can reduce oxidized Mge1 and more specifically the oxidized Met at position 155 in Mge1. MALDI-TOF MS/MS was used to investigate whether Mxr2 targets the oxidized Met-155 for reduction. We repeated the MALDI-TOF analysis of H_2O_2-treated Mge1 protein but with one modification. After H_2O_2 treatment, Mge1 was further treated with DTT in the presence or absence of Mxr2. As shown in Figure 3E, H_2O_2-treated Mge1 in the absence of Mxr2 was >75% enriched in the higher–*m/z* peak of 2659.3, indicating that H_2O_2 was able to efficiently oxidize Mge1 (Figure 3E). Of most importance, Mxr2 treatment reduces the intensity of the oxidized *m/z* 2659.3 peak by nearly 50% concomitant with a corresponding increase in the intensity of the unoxidized peak of *m/z* 2643.3 (Figure 3F).

To determine whether Mxr2 activity on oxidized Mge1 is comparable to any other known substrates of Mxr2, we adopted a coupled NADPH-dependent thioredoxin/thioredoxin reductase assay system (Tarrago *et al.*, 2012). Oxidized wild-type recombinant Mge1, free methionine sulfoxide (as a negative control), and glutathione *S*-transferase (GST; a known Mxr2 substrate protein) were used as substrates. Equimolar amounts of purified wild-type Mge1 and GST were treated with H_2O_2 for 4 h before addition of Mxr2 in a coupled assay as described in *Materials and Methods*. Mxr2 exhibits significant activity on H_2O_2-treated Mge1 that is comparable to its activity on H_2O_2-treated GST (Figure 4A). However, Mxr2 shows very much less activity on free methionine sulfoxide, indicating the specificity of Mxr2 to reduce oxidized Mge1 and GST. Our results clearly show that Mge1 is a substrate for Mxr2, and Mxr2 significantly and specifically acts on oxidized methionine at position 155 in Mge1.

Because the results described unequivocally show that Mxr2 reduces oxidized Mge1 specifically, we further sought to see whether there is any correlation with the functional activity of Mge1. In an earlier study, we showed that dimeric Mge1 interacts with Hsp70 to form Hsp70-Mge1 complex, which has a stimulatory effect on the ATPase activity of Hsp70. We also showed that H_2O_2 reduces this stimulatory function of Mge1 (Marada *et al.*, 2013). To determine whether oxidation of methionine 155 within Mge1 is directly responsible for its loss of stimulatory activity and whether the reducing activity of Mxr2 on Mge1 will restore this function, we examined the steady-state in vitro ATPase activity of Hsp70 as described in *Materials and Methods*. Mitochondrial Hsp70 has low ATPase activity in the absence of Mge1 (Figure 4B). In the presence of wild-type recombinant Mge1, the ATPase activity of mHsp70 is enhanced threefold. However, H_2O_2-treated Mge1 has a negligible effect on the ATPase activity of mHsp70. Most important, prior treatment of oxidized Mge1 with Mxr2 restores the ATPase-stimulatory activity of Mge1 on Hsp70 in vitro (Figure 4B).

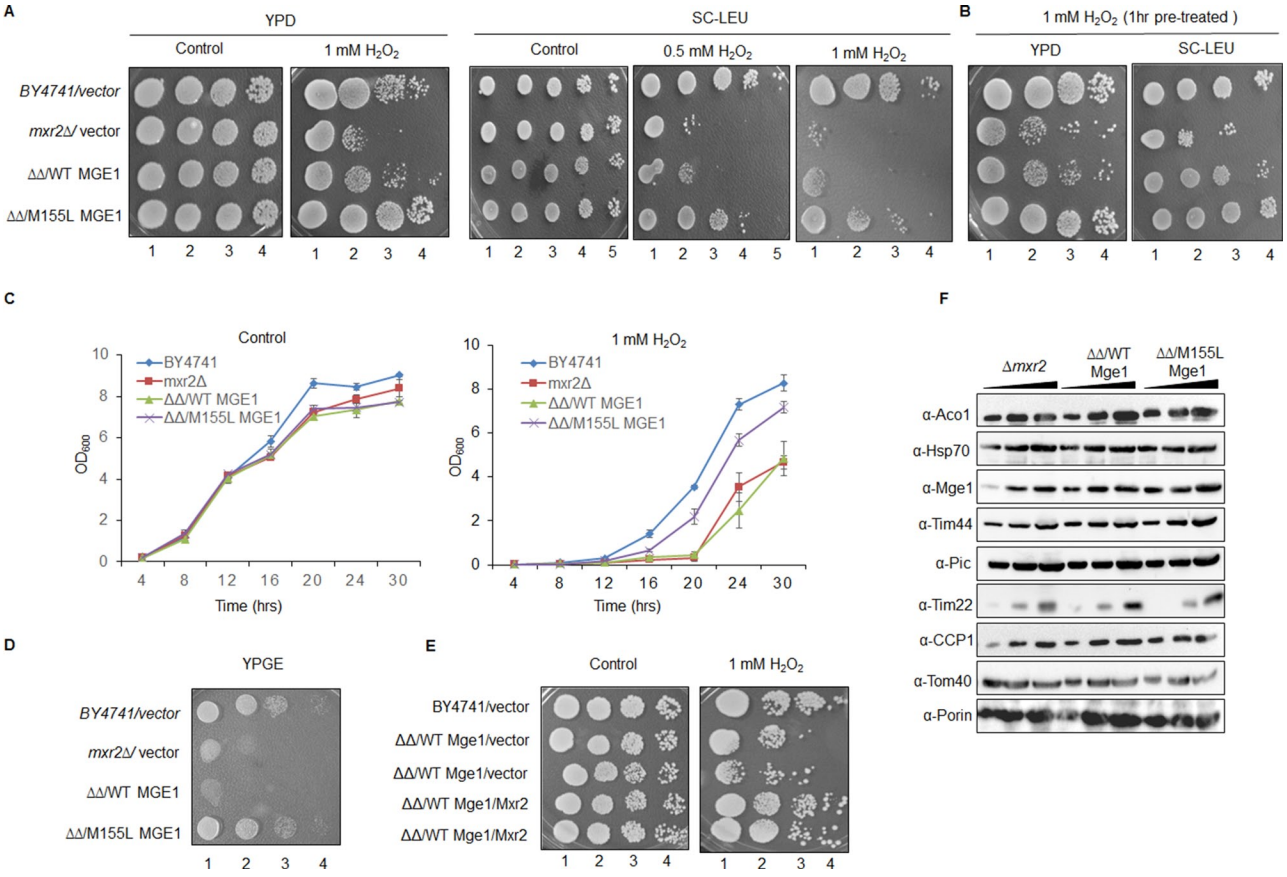

FIGURE 5: Mge1 is a physiological mitochondrial substrate of Mxr2. Yeast strains yNB62 (BY4741/vector), yNB115 (*mxr2*Δ), yNB130 (ΔΔ/WT MGE1), yNB131 (ΔΔ/M155L MGE1), yNB122 (mxr2Δ/vector), yNB132 (ΔΔ/WT MGE1/vector), and yNB133 (ΔΔ/WT MGE1/Flag-Mxr2) were studied for growth on solid and liquid media under stress conditions. (A, B, D) Spotting assay. All strains were grown overnight in YPD medium before being serially diluted for cells from strains yNB62, yNB115, yNB130, and yNB131 and spotted on YPD ± (A), SC-Leu ± 0.5 mM/1 mM H_2O_2 (A, middle), and YPGE (D) plates. (B) All strains were grown to mid log phase, treated with 1 mM H_2O_2, and spotted on YPD or SC-Leu plates. (C) Growth curve. Yeast strains were grown overnight in YPD medium and used to inoculate fresh YPD medium supplemented with or without H_2O_2. Growth was monitored by taking $OD_{600\ nm}$ every 4 h over a 30-h time period. (E) Overnight-grown yeast cells from the strains yNB62, yNB130, and yNB131 were spotted on YPD plates with or without 1 mM H_2O_2. (F) Mitochondria were isolated from indicated strains, and increasing concentrations of the mitochondrial fraction (10, 25, and 50 µg) were resolved on SDS–PAGE and subjected to immunoblot analysis using antibodies against mitochondrial proteins. (ΔΔ indicates the chromosomal deletion of both MXR2 and MGE1.)

The aforementioned results clearly show that Mge1 is oxidized at Met-155 in the presence of H_2O_2, and Mxr2 specifically reduces the oxidized Met-155 in Mge1 in vitro. We additionally provide evidence that Mge1 is a substrate for Mxr2 and that Mxr2 specifically reduces oxidized methionine at position 155 in Mge1 and modulates mHsp70 function.

Mge1 is a physiological substrate of Mxr2

To determine whether Mge1 is a physiological substrate of Mxr2 and if so, to elucidate the in vivo functional significance of Mge1 MetO reduction by Mxr2, we studied the effect of deletion of MXR2 on the growth of yeast strains expressing either wild-type MGE1 or MGE1 M155L mutant. Because Mge1 is an essential gene, we constructed haploid yeast strains that had chromosomal copies of both MGE1 and MXR2 deleted (indicated by ΔΔ) but ectopically expressed either wild-type (WT) MGE1 (yNB130:ΔΔ/WT MGE1) or MGE1 M155L mutant (yNB131:ΔΔ/M155L MGE1) from high-copy plasmids. The parent BY4741 strain and its derivatives yNB66 (BY4741/vector) and yNB122 (*mxr2*Δ, vector) were included as controls when testing for growth. We compared the growth-sensitive phenotype of all the foregoing yeast strains by spotting on YPD and synthetic complete (SC)-Leu plates that were supplemented with or without H_2O_2 (see later discussion of Figure 6A). All the strains had comparable growth on YPD and SC-Leu plates. However, the growth of WT MGE1–expressing strains in *mxr2*Δ background were severely retarded in the presence of H_2O_2 compared with the parent BY4741 strain, which has an intact MXR2 (Figure 5A). Most important, yNB131 strain expressing MGE1 M155L in the MXR2 deletion background was able to grow robustly in the presence of H_2O_2. Similar results were obtained when yeast cells were grown to mid log phase and treated with H_2O_2 for 1 h before spotting on YPD or Sc-Leu plates (Figure 5B). Further, we observed similar results when the aforementioned yeast strains were grown in liquid YPD in the presence or absence of H_2O_2 (Figure 5C). Our results suggest that MGE1 and MXR2 have a functional genetic interaction and that MXR2 is epistatic to MGE1. It was shown previously that deletion of MXR2 compromises the growth of yeast on media containing nonfermentable carbon sources (Kaya *et al.*, 2010). To examine whether MGE1

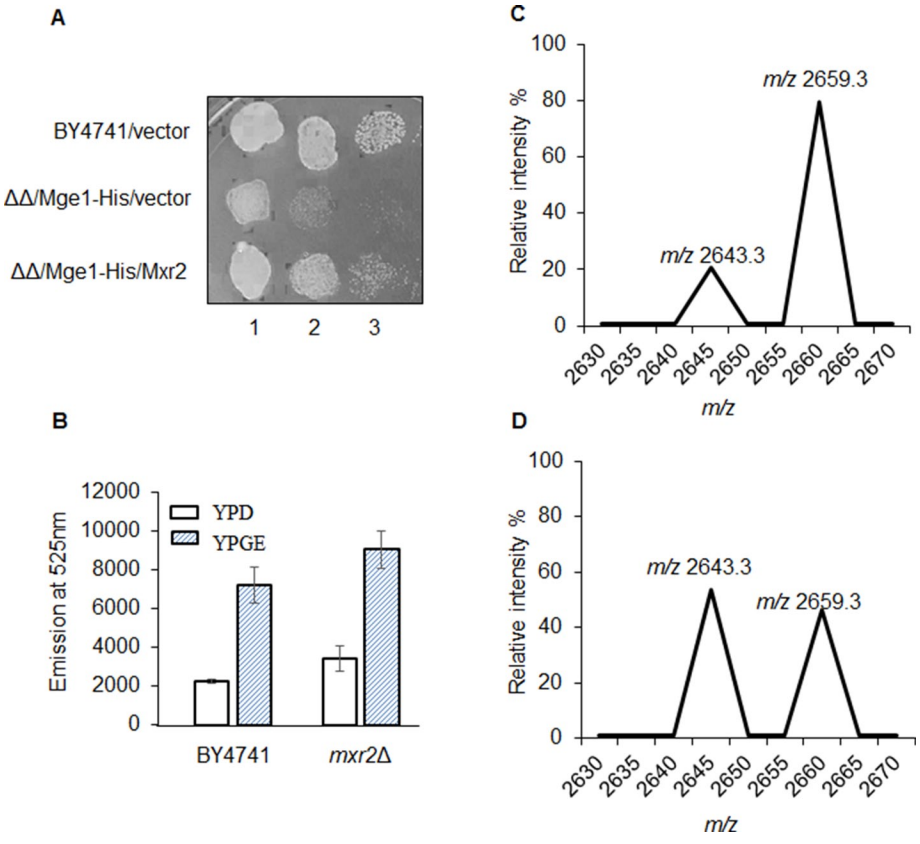

FIGURE 6: MALDI-TOF spectrum of Met-155 peptide of intracellular His-Mge1. (A) Yeast strains BY4741, yNB134 (ΔΔ/His-MGE1), and yNB135 (ΔΔ/His-MGE1/Flag-MXR2) were grown overnight in YPD medium serially diluted by 10-fold, and spotted on YPGE plates. (B) Yeast strains BY4741 and yNB115 were grown to early log phase either in YPD or YPGE, and equal amount of cells were used to measure the ROS as mentioned in *Materials and Methods*. The histogram represents the average emission values of DCFDA at 525 nm from three replicates. (C, D). Reconstructed MALDI-TOF spectrum of His-Mge1 in vivo. Yeast strains YNB134 and yNB135 were grown in YPGE medium, and His-Mge1 was purified using Ni-NTA beads and subjected to MALDI-TOF analysis as described in *Materials and Methods*. MALDI-TOF spectra of the Met-155 containing peptide of His-Mge1 from yNB134 (C) and yNB135 (D) . The peak with *m/z* value 2643.3 represents the unoxidized Met-155 peptide, and the peak with *m/z* value of 2659.3 represents the oxidized Met-155 peptide as deduced from the MS/MS spectrum (Supplemental Figure S6).

M155L mutant can rescue this growth defect, we tested the growth of yNB66, yNB122, yNB130, and yNB131 strains on YPGE plates, which contain ethanol and glycerol as nonfermentable carbon sources. As shown in Figure 5D, overexpression of MGE1 M155L mutant rescues the growth defect of *mxr2*Δ strain compared with the *mxr2*Δ strain expressing wild-type MGE1 on YPGE plates. We additionally transformed yNB130 with a high- copy URA3 vector or with pNB475 to create yNB132 (ΔΔ/WT MGE1, vector) and yNB133 (ΔΔ/WT MGE1, FLAG-MXR2) strains, respectively, to check whether ectopic expression of MXR2 can compensate the chromosomal deletion of MXR2. Ectopic expression of MXR2 is able to compensate the chromosomal deletion of MXR2, as strain yNB133 displayed better growth than yNB132 in the presence of H_2O_2 (Figure 5E).

To rule out the possibility that altered protein expression might be responsible for the resistance offered by MGE1 M155L expression in the absence of MXR2, we evaluated the steady-state level of mitochondrial proteins in yNB122 (*mxr2*Δ), yNB130 (ΔΔ/WT MGE1) and yNB131 (ΔΔ/MGE1 M155L) strains. Isolated mitochondrial samples were resolved on SDS–PAGE, Western transferred, and probed with antibodies specific for porin, Tim44, mHsp70, Tim22, CCPO, aconitase, Tim23, and Tom40 (Figure 5F). We did not observe any significant change in the expression of the tested proteins. Taken together, the results show that MGE1 M155L is not susceptible to oxidation and thereby overcomes the requirement of MXR2 by the yeast cell to grow in the presence of oxidative stress.

In vivo oxidation of Mge1

To ascertain whether Mge1 is indeed being oxidized at methionine 155 in vivo and subsequently reduced by Mxr2, we constructed two yeast strains, yNB134 (ΔΔ/His-MGE1) and yNB135 (ΔΔ/His-MGE1, Flag-MXR2) as described in *Materials and Methods*. Yeast strains yNB134 and yNB135 were spotted on YPGE plates. As expected, yeast strain yNB134 has very poor growth on YPGE plates. However, yNB135 exhibits better growth, as Flag-MXR2 is apparently able to compensate for the MXR2 deletion (Figure 6A). Further, we observed that the internal ROS is much higher when cells are grown in nonfermentable carbon medium (YPGE) than with YPL/YPD medium (Figure 6B).

Yeast strains yNB134 and yNB135 were grown in liquid YPGE medium, and His-Mge1 was affinity purified by passing the yeast cell extract through a Ni-NTA column as described in *Materials and Methods*. Purified His-Mge1 was resolved on SDS–PAGE and stained with Coomassie, and the His-Mge1 protein band was extracted from the gel for MALDI-TOF MS/MS analysis as described earlier. The relative mass spectra of His-Mge1 from strains yNB134 and yNB135 are similar (Supplemental Figure S5). MALDI-TOF analysis revealed that in the absence of MXR2, the Met-155 containing peptide of Mge1 exists in both oxidized (*m/z* 2659.3) and unoxidized (*m/z* 2643.3) forms (Figure 6C). However, the relative intensity of the oxidized peak is much higher than the unoxidized peak in the case of the Met-155 peptide from yNB134, which lacks MXR2. In contrast, the reverse is true for yNB135, which ectopically expresses Flag-MXR2. Of interest, this result shows that the internal ROS generated during growth in YPGE medium is sufficient to trigger oxidation of Mge1. Nevertheless, the MALDI-TOF results are consistent with the slow-growth phenotype of yNB134 strain (ΔΔ/His MGE1) on YPGE plates and our coimmunoprecipitation results, which showed that Mge1 interacts with Mxr2 in vivo (Figure 2E). Most important, ectopic expression of MXR2 is able to reduce the oxidized form of His-Mge1, as there is an increase in the intensity of the unoxidized Met-155 peptide (*m/z* value 2643.3) concomitant with a decrease in the Met-155 oxidized peptide (*m/z* value 2659.3; Figure 6D). We further confirmed the oxidation status of the Met-155 peptide by MS/MS analysis using protein isolated from the foregoing strains (Supplemental Figure 6, A and B). Consistent with our in vitro findings, we find that Mge1 indeed is capable of being oxidized at Met-155 in vivo. Of greatest note, we show through genetic complementation experiments and by MALDI-TOF MS/MS that expression of MXR2 is essential for restoring growth during oxidative stress and for reducing oxidized Mge1 at Met-155.

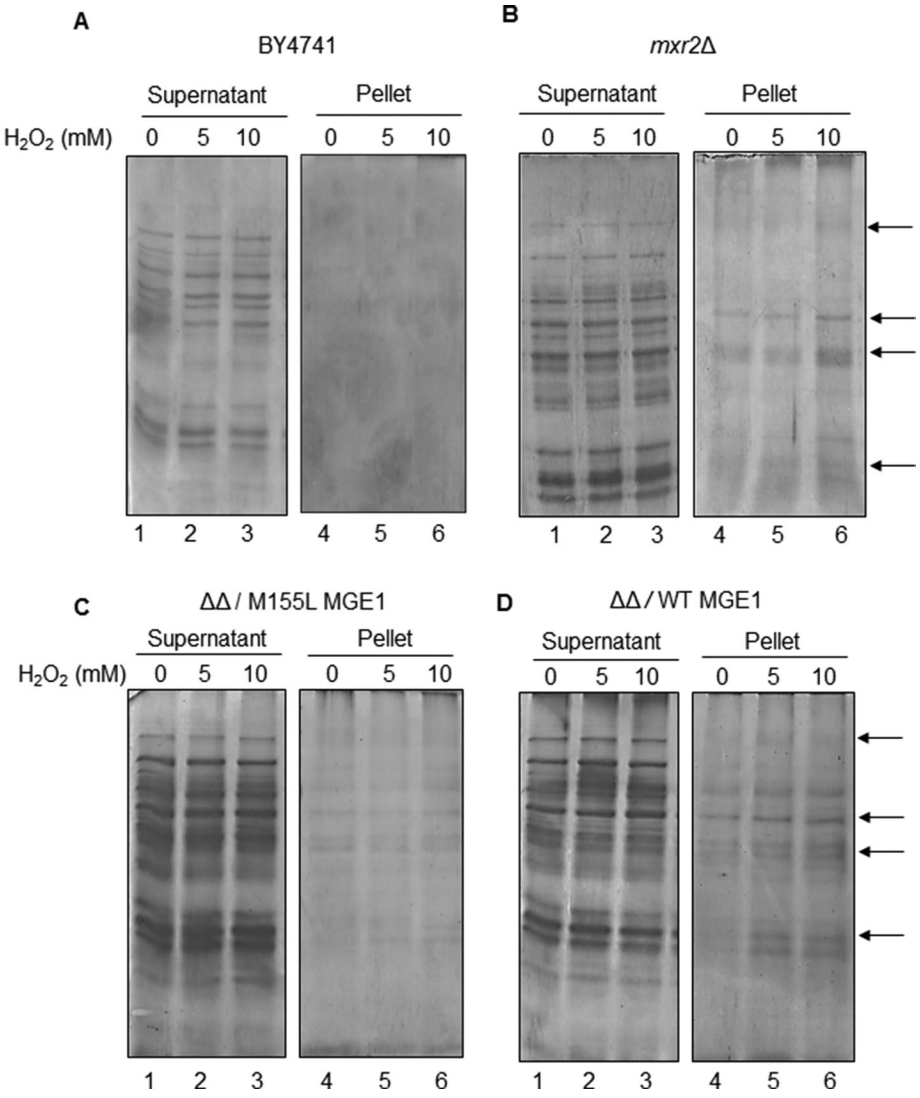

FIGURE 7: Oxidative modification of WT Mge1 causes loss of function. (A–D) Mitochondria (50 µg) were isolated from strains BY4741, yNB115 (*mxr2*Δ), yNB130 (ΔΔ/M155L Mge1), and yNB131 (ΔΔ/WT Mge1) and treated with increasing concentrations of H_2O_2 in the presence of energy as indicated and processed as in *Protein aggregation assay* in *Materials and Methods*. Images of silver-stained SDS–PAGE gels of supernatant (lanes 1–3) and pellet fractions (lanes 4–6) of mitochondria.

Mge1 M155L protects cells from stress-mediated protein aggregation

To understand the functional consequence of Mge1 Met-155 oxidation in the absence of MXR2, we monitored protein aggregation in strains that express wild-type MGE1 or MGE1 M155L mutant in an MXR2-deletion background. Most of the proteins have a finite tendency to misfold or unfold during stress conditions and form protein aggregates. Oxidative stress in the form of H_2O_2 can induce aggregation of proteins in mitochondria. The evidence has implicated Mge1 in the role of an oxidative sensor, modulator of Hsp70, and regulator of mitochondrial protein import. In addition, Mge1 also acts as a cochaperone for Ssq1, a homologue of Hsp70 that is involved in the biogenesis of Fe-S clusters and also in protein folding (Langer *et al.*, 1992; Westermann *et al.*, 1995; Lutz *et al.*, 2001). Of interest, Fe-S– containing proteins are readily prone to oxidation (Beinert *et al.*, 1997). We sought to examine the role of Mge1 M155L mutant in the prevention of aggregation of proteins during oxidative stress. Toward this end, we used two strains, BY4741 as control and a second strain, yNB115, which is deleted for MXR2. Strains BY4741 and yNB115 were grown in YPL medium for 24 h before harvesting the cells. Mitochondria were isolated from both the strains and treated with increasing concentration of H_2O_2 (0, 5, 10 mM) for 30 min in the presence of energy before centrifuging the samples. ATP-dependent Hsp70 activity is inhibited when energy is not present, and it is likely that any differences in protein aggregation will be masked by this low activity (Hartl *et al.*, 2011). Hence energy in the form of ATP was included. The supernatant and pellet fractions were resolved on SDS–PAGE and silver stained, and the protein profile was examined (Figure 7A) for protein aggregation. Absence of MXR2 triggers increased protein aggregation compared with control sample in the pellet fraction even at low concentration of H_2O_2 (Figure 7B). We repeated the experiment in strains ectopically expressing either MGE1 M155L mutant (yNB131) or MGE1 (yNB130) wild type in MXR2-deletion background (Figure 7, C and D). We find that the mitochondria isolated from the strain harboring MGE1 M155L mutant is partially protected from protein aggregation (Figure 7C). In the case of mitochondria from the strain carrying wild-type MGE1, protein aggregation is observed even at 5 mM H_2O_2. These results indicate that the oxidation-resistant Mge1 M155L mutant prevents protein aggregation.

Our findings provide compelling evidence that Mge1 and Mxr2 are components of the oxidative response pathway and that Mxr2 is epistatic to Mge1. We presented genetic and biochemical evidence to show that Mge1 is a physiological substrate of Mxr2. MGE1 M155L mutant can effectively compensate for the absence of MXR2, as it relieves the growth defect associated with MXR2 deletion in the presence of H_2O_2 and on nonfermentable carbon sources. Most importantly, we have shown that Met-155 in Mge1 is oxidized in vitro and in vivo and that Mxr2 very specifically can reduce oxidized Met-155 within Mge1. We conclude that oxidized Mge1 is a substrate of Mxr2 and that methionine 155 is crucial for the reversible regulation of Mge1, adding a new paradigm to the regulation of the oxidative stress response pathway.

DISCUSSION

Oxidative stress causes an imbalance in the redox potential that may lead to the development of several neurological disorders and ageing (Moskovitz, 2005). Several antioxidative defensive mechanisms have evolved to neutralize oxidative stress and protect cells from oxidative damage (Meyer *et al.*, 2009; Pamplona and Costantini, 2011). Greater than 90% of cellular oxygen is consumed within mitochondria, making mitochondria the main contributor of ROS and mitochondrial proteins as major and immediate targets of ROS

(Finkel and Holbrook, 2000; Orrenius *et al.*, 2007; Murphy, 2009). ROS generated in mitochondria has been implicated in multiple signaling pathways ranging from apoptosis and tumor survival to turnover of mitochondria, also known as autophagy. Increasing evidence suggests that ROS is also essential for several biological processes, such as growth and development (Finkel and Holbrook, 2000; Winterbourn and Hampton, 2008). Sulfur-containing amino acids methionine and cysteine are easily susceptible to oxidation, thereby placing the cell on alert. This mechanism plays an important role in regulating protein function and redox signaling. Like cysteine, hydrophobic methionine is also capable of being oxidized to create a hydrophilic environment within its proximity with an increased affinity for hydrogen bonding. Hydrogen bonding causes a conformational change in the proteins. The reversibility of the oxidation status of Cys and Met amino acids in a protein transforms these amino acids into powerful regulators of the protein's function and also regulate the interaction of the protein with its partners (Levine *et al.*, 2000; Winterbourn and Hampton, 2008). Of interest, yeast Mge1 harbors only one methionine, and this is present in the helical region of the protein. Substitution of methionine to leucine renders the Mge1 protein resistant to oxidation and is also sufficient to stabilize the dimer formation and interaction with Hsp70 both in vitro and in vivo from oxidative stress (Marada *et al.*, 2013).

Mge1-mediated ADP release is the rate-limiting step in the exchange of ADP for ATP by Hsp70. Presence of Mge1 increases this nucleotide exchange activity of Hsp70 by 5000-fold (Packschies *et al.*, 1997). The Mge1 dimer has two long α-helices, a four-helix bundle, and six β-strands. The α-helical bundles are essential for dimer formation, besides providing a surface for Mge1-Hsp70 interaction (Mehl *et al.*, 2003). The amino acids present on the exterior surface of the four α-helical bundles are uniquely exposed to high solvent content (Harrison *et al.*, 1997). Impaired Mge1 dimer formation and failure to interact with Hps70 contributes to the lowered efficiency of Hsp70 (Wu *et al.*, 1994). Intriguingly, the Met-155 resides in this four–α-helical bundle motif. Our in vitro results shown that oxidation of Met-155 decreases interaction of Mge1 with Hsp70 and decreases Hsp70 ATPase activity (Figure 4B). Hence we believe that the four–α-helical region is crucial for oxidation sensor activities of Mge1 for regulating Hsp70 function.

Methionine sulfoxide reductases are important regulators of oxidative stress. Oxidation of methionines in proteins alerts these reductases to reduce the oxidized proteins and thereby protect the function of proteins and the cell from oxidative damage. Although mitochondrial proteins have been known to be major targets of ROS, there have been no reports on the functional regulation of these proteins by methionine oxidation. The present study underscores the importance of the mitochondrially localized MXR2, as yeast cells devoid of MXR2 are sensitive to H_2O_2 stress. In yeast, deletion of cytosol-localized MXR1 also leads to dysfunctional mitochondria (Kaya *et al.*, 2010). Yeast deleted for MXR1 are only sensitive to H_2O_2 at higher concentrations (not shown), whereas deletion of MXR2 results in increased sensitivity even at low concentration (Figure 1A). Intriguingly, yeast having double deletion of MXR1 and MXR2 are much more sensitive to H_2O_2 than yeast harboring only MXR2 deletion (Supplemental Figure S1). We suspect that Mxr1 might have a role in regulating the cytosolic redox balance and thereby indirectly affect mitochondrial function. The isoforms of reductases have increased with evolution, underlining their increased requirement (Zhang and Weissbach, 2008). In higher eukaryotes, both Mxr1 and Mxr2 isoforms are present in mitochondria, indicating the presence of multiple substrates and increased complexity in regulation of redox homeostasis. HMGE, the human homologue of Mge1, is similarly sensitive to H_2O_2 (Marada *et al.*, 2013). To our knowledge, Mge1 is the first in vivo substrate of mitochondrial Mxrs. We also showed that the function of Mge1 is reversibly regulated by oxidation/reduction status of its methionine-residue present in the four–α-helical bundle motif (Figures 3 and 4).

The Hsp70 complex (DnaK70-DnaJ-GrpE, prokaryotic homologues) laterally with GroEl/GroEs chaperonins increases the efficiency of protein folding and prevents misfolded proteins, which leads to aggregation (Langer *et al.*, 1992; Westermann *et al.*, 1995), whereas prokaryotic chaperone ClpB, in association with DnaK, the prokaryotic homologue of Hsp70, binds large aggregate of proteins and dissociates them into smaller aggregates or individual proteins. The small aggregates are further dissolved by the former system. In addition to protein folding, dissociation of the aggregated protein requires energy in the form of ATP, as the Hsp70 system and the other components of the chaperone system are otherwise in the switch-off mode (Hartl *et al.*, 2011; De Los Rios and Goloubinoff, 2012). In the absence of Mxr2, the oxidative-resistant mutant of Mge1 (M155L) stalls protein aggregation to a certain extent in the presence of energy (Figure 7). These results lend further support to our conclusion that oxidation of Met-155 in Mge1 causes loss of function of the Mge1-Hsp70 complex and this is manifested as an oxidative-sensitive phenotype in the *mxr2*Δ strain, which has wild-type Mge1, in the presence of H_2O_2. The substitution of methionine to leucine at position 155 in Mge1 is a gain-of- function mutation, as it is able to protect yeast cells deleted for *mxr2*Δ from oxidative stress to a certain level. In addition, Mge1 function is essential for the Ssq1-mediated Fe-S cluster biogenesis pathway (Knight *et al.*, 1998; Lutz *et al.*, 2001; Uzarska *et al.*, 2013). Further, it is known that Mge1 plays a role in degradation of misfolded proteins, protein folding, and protein sorting (Savel'ev *et al.*, 1998; Chacinska *et al.*, 2009; Iosefson *et al.*, 2012). Hence a stable Hsp70-Mge1 complex may not be the only reason for the effect of the Mge1 M155L mutant on protein aggregation. Given the vulnerability of the Fe-S–containing proteins to oxidation, it would be of interest to study the interplay of Mxr2 and Mge1 in the biogenesis of Fe-S clusters.

Because Mge1 has multifunctional roles, it is important that a small perturbation in ROS levels should not alter the functions of Mge1. Most likely, the cell uses Mxr2 to reduce any oxidized Mge1 so that Mge1-dependent pathways operate smoothly and continuously. The cell may be using the reversible modification of the methionine residues in such proteins to revert to normalcy rapidly once the stress is released. It is possible that such a mechanism operates during heat, cold, and other stresses besides the oxidative stress that has been described here. Thus the oxidative stress response pathway mediated by Mge1 and Mxr2 will eventually help in identifying additional components involved in redox biology and in developing therapeutics for oxidative stress–mediated diseases.

MATERIALS AND METHODS

Plasmid construction

The primers and plasmids used in this study are listed in Supplemental Tables S2 and S3, respectively. The complete coding sequence of yeast MXR2 (Δ29 amino acids, without mitochondrial presequence) was amplified using yeast genomic DNA as a template with the primer pair MXR2_Fwd2 (5′-AAA ACC ATG GGC AAG AGC AAG AAA ATG AGT-3′)/MXR2_Rev2 (5′-ACCC AAGCTT ATC CTT CTT GAG GTT TAA AGA-3′). The amplified MXR2 product was cloned into *Escherichia coli* expression vector pET28a$^+$ to generate pNB483 with hexahistidine tag at the C-terminus of MXR2. To create plasmid pNB485, which harbors MXR2 (Δ29 amino acids), without any tag, MXR2 was amplified using primers MXR2_Fwd2/MXR2_Rev4

(5′-ACCC CTCGAG TTA ATC CTT CTT GAG GTT TAA-3′) from yeast genomic DNA and cloned as *Nco*I-*Xho*I fragment into pet28a^{+} vector. Complete coding sequence of MXR1 was amplified from yeast genomic DNA with primers MXR1_Fwd1 (5′-AAAC GAATTC ACC ATG TCG TCG CTT ATT TCA-3′) and MXR1_Rev1 (5′-ACCC CTC-GAG CTA CAT TTC TCT CAG ATA ATG-3′) and cloned into pcDNA 3.1 to generate pNB467. MXR2 full length was amplified from yeast genomic DNA with primers using MXR2_Fwd4 (5′-AAAC GAA TTC ACC ATG AAT AAG TGG AGC AGG-3′)/MXR2_Rev4 and cloned into pcDNA 3.1 to generate pNB468.

To create a plasmid carrying FLAG-MXR2, full-length MXR2 was initially amplified with primers MXR2_Fwd4/MXR2_Rev5 (5′-ACCC AAGCTT ATC CTT CTT GAG GTT TAA AGA-3′) and cloned into pTEF-2 μ-URA to generate pNB472. pNB472 was digested with *Hin*dIII/*Xho*I restriction enzymes and a FLAG epitope inserted therein to generate plasmid pNB475. FLAG epitope linker was created with predigested primers FLAG_Fwd6 (5′-AG CTT GAC TAC AAG GAC GAT GAT GAC AAG GAC TAC AAG GAC GAT GAT GAC AAG CTA C-3′) and FLAG_Rev6 (5′-TC GAG TAG CTT GTC ATC ATC GTC CTT GTA GTC CTT GTC ATC ATC GTC CTT GTA GTC A-3′).

Plasmid pNB579 (pTEF MGE1-HIS6, 2 μ, LEU) is a high-copy yeast shuttle vector harboring the His tag at the C-terminus of MGE1. To construct pNB579, full-length MGE1 was amplified with primers MGE1_Fwd7 (5′-CCCC GGATCC ACC ATG AGA GCT TTT TCA GA GCC-3′)/MGE1_Rev7 (5′-AAT T CTC GAG TTA GTG GTG GTG GTG GTG GTG GTG CCA TGG AAT GTT CTC TTC GCC CTT AAC-3′) and cloned into pTEF 2 μ, LEU vector. Plasmids containing thioredoxin (Trx) and thioredoxin reductase (TrxR) were kind gifts from Charles Williams (University of Michigan Medical School, Ann Arbor, MI).

Expression and purification of recombinant proteins

E. coli BL21 (DE3) CodonPlus-RIL cells were transformed with pNB483 plasmid carrying HisMXR2. Recombinant protein expression was induced with 1 mM isopropyl-β-D-thiogalactoside (IPTG), and soluble protein was purified using Talon metal affinity resin (GE Healthcare, Uppsala, Sweden) and dialyzed in phosphate-buffered saline (PBS), pH 7.2, with 5 mM β-mercaptoethanol. pNB485 plasmid was transformed into *E. coli* BL21 (DE3) Codon Plus-RIL, and untagged MXR2 protein was expressed by inducing bacterial cultures with 1 mM IPTG; the soluble protein fraction was stored in PBS at −20°C. Native untagged Trx and TrxR proteins were expressed in *E. coli* BL21 (DE3) Codon Plus-RIL as described (Lennon and Williams, 1995), and the soluble extracts were passed through a DEAE cellulose column. The column was washed with buffer and protein eluted with increasing concentration of NaCl. Eluted sample containing high fractions of Trx and TrxR were used for further steps. The eluted proteins were concentrated and dialyzed against PBS with 10% glycerol. Wild-type, mutant Mge1, and Hsp70 proteins were expressed and purified as described (Marada *et al.*, 2013).

Yeast strains and construction

Yeast strains used in this study and their genotypes are shown in Supplemental Table S1. Yeast strains used in this study were derivatives of BY4741 or BY4742. Haploid yeast strains yNB114 and yNB115 deleted for MXR1 and MXR2, respectively, were purchased from EUROSCARF (Frankfurt, Germany). The construction of haploid yNB65 strain deleted for chromosomal MGE1 but expressing MGE1 ectopically from plasmid pNB65 (pTEF-MGE1, 2 μ, URA3) has been previously described (Marada *et al.*, 2013). Diploid yNB118 strain heterozygous for MGE1 and MXR2 was constructed by mating the haploid yNB65 strain with haploid yNB115. Standard yeast genetic methods were used to sporulate diploid yNB118 on SC-URA, and the dissected haploid spores were screened for double deletion of chromosomal MGE1 and MXR2 by PCR using primers MGE1_Fwd8, MXR2_Fwd9, and KAN_REV. For the yNB126 strain, denoted ΔΔ, a haploid progeny contains deletion for both chromosomal genes of MGE1 and MXR2. pNB186 (pTEF-MGE1, 2 μ, LEU2) and pNB187 (pTEF- MGE1 M155L, 2 μ, LEU2) were transformed into yNB126 to generate yNB128 and yNB129 strains, respectively. The URA3 plasmid pNB45 was evicted from yNB128 and yNB129 strains by growing them on SC plates supplemented with 5-fluoroorotic Acid (5-FOA) plates to generate yNB130 and yNB131 strains, respectively. The strains were confirmed by their inability to grow on SC-URA plates. Strain yNB115 was transformed with plasmid pNB475 to create strain yNB124. Strain yNB115 was transformed with pNB402 (pTEF, 2 μ LEU2) vector to generate strain yNB122. The strain yNB134 expressing His-MGE1 was created by plasmid shuffling pNB579 (pTEF-MGE1-His6, 2 μ, LEU2) into yNB126 as described. Yeast strain yNB140 double deletion for MXR1 and MXR2 was constructed from haploid mxr1Δ and mxr2Δ strains. Briefly, the diploid strain obtained from mating of mxr1Δ and mxr2Δ was sporulated. Haploid strains were screened with selected markers and PCR using primers MXR1_Fwd10, MXR2_Fwd9, and KAN_REV to confirm the double deletion of MXR1 and MXR2.

Yeast media and growth conditions

Yeast *S. cerevisiae* was grown in standard YPD medium containing 1% yeast extract, 2% peptone, and 2% dextrose unless otherwise stated. For retaining the plasmids, yeast strains were grown in SC medium containing yeast nitrogen base (YNB) with all amino acids except uracil (SC-Ura) or leucine (SC-Leu). Synthetic medium was prepared as follows: 2% dextrose and 0.67% SC medium, with pH was adjusted to 5.5 with NaOH. Nonfermentable carbon source medium had either 2% lactic acid (YPL) or 3% glycerol and 2% ethanol (YPGE) instead of dextrose in YPD. To evict URA3 plasmid, strains were grown on SC medium containing 5-FOA (0.67% SC-Ura, 2% dextrose, 60 μg/ml uracil, 2% agar, and 0.1% 5-FOA). Yeast transformation was done by the LiOAc chemical method (Gietz and Woods, 2002). Yeast strains were grown at 30°C with shaking.

Spotting assay

Freshly streaked yeast cultures were grown overnight in YPD or SD medium and normalized to OD_{600} of 0.5. A 10 μl amount of each dilution was spotted on YPD or SC-Leu containing various concentrations of H_2O_2 as indicated in the legends, and plates were incubated at 30°C for 2 d. Spotting assay that was carried out on YPGE plates incubated at 30°C for 4–5 d. Growth curve experiments were performed in YPD medium with starting OD_{600} of 0.02. The inoculum for the growth curve was taken from overnight cultures grown in YPD. The cultures for monitoring growth rate were grown at 30°C in the presence or absence of H_2O_2, and OD_{600} was monitored at regular intervals. Growth of each strain was carried out in triplicate by taking three different colonies for culture, and the average was calculated for each time point.

Isolation of mitochondria

Yeast strains were grown in YPL/YPGE medium at 30°C, and cells were harvested when the cultures reached OD_{600} of 1 or 2. Cultures were centrifuged at 5000 rpm for 5 min, and the cell pellets washed with autoclaved distilled water. The cells were treated with 10 mM dithiothreitol (DTT) in 0.1 M Tris-SO_4, pH 9.4, buffer for 15 min and centrifuged at 5000 rpm for 5 min. Cells were

converted to spheroplasts by using Zymolyase in 1.2 M sorbitol/20 mM phosphate buffer, pH 7.0. After obtaining 50% lysis of cells (lysis correlated to a decrease in OD_{600} of 100 µl of cells in 900 µl of water), the resulting spheroplasts were gently washed with 1.2 M sorbitol two or three times. The spheroplasts pellets were suspended in SEM buffer (250 mM sucrose, 1 mM EDTA, 10 mM 3-(*N*-morpholino)propanesulfonic acid [MOPS], 1 mM phenylmethylsulfonyl fluoride, 0.2% bovine serum albumin [BSA], pH 7.0) and homogenized using a Dounce homogenizer (15 times). The homogenates were centrifuged at 3500 rpm. The supernatants were collected and centrifuged at 10,000 rpm for 10 min. The resultant pellets were dissolved in SEM buffer and centrifuged at 3500 rpm for 5 min. The supernatants were once again centrifuged at 10,000 rpm for 10 min and pellets washed three times in SEM buffer. The mitochondria were solubilized to a concentration of 1 mg/ml in SEM buffer (without BSA) and kept frozen at −80°C.

In vitro protein import

The ^{35}S-radiolabeled full-length proteins Mxr1, Mxr2, and Su9-DHFR were generated using a T7 or Sp6 in vitro–coupled transcription translation system (Promega, Madison, WI). A 100-µg amount of mitochondria was suspended in import buffer (0.2% fatty acid–free BSA, 250 mM sucrose, 80 mM KCl, 5 mM $MgCl_2$, 5 mM MOPS, pH 7.0, 5 mM ATP, and 1 mM DTT) and treated with valinomycin (5 µM) for 15 min. Next ^{35}S-labeled proteins were added and incubated at 30°C for 20 min. After import, each import sample was divided into two equal halves. One half was treated with trypsin (50 µg/ml) for 15 min on ice, and the other half was processed directly. Trypsin inhibitor was added to the import sample after the trypsin treatment. The samples were washed with SEM buffer, solubilized in 2× sample buffer, resolved on an SDS–PAGE gel, and analyzed by autoradiography.

Preparation of mitoplasts and treatment with proteinase K

A 100-µg amount of yeast mitochondria was suspended in hypotonic buffer (20 mM KCl, 10 mM 4-(2-hydroxyethyl)-1-piperazineethanesulfonic acid, pH 7.2) and incubated for 20 min with occasional mixing on ice, followed by a spin at 10,000 rpm, 10 min at 4°C to generate mitoplasts as pellet. Mitoplasts were collected and resuspended in SEM buffer. Mitochondria, mitoplasts, and 0.1% Triton X-100–solubilized mitochondrial extract were treated with or without proteinase K (50 µg/ml) in SEM buffer. After incubation for 10 min on ice, PMSF (1 mM) was added and the samples centrifuged at 10,000 rpm for 10 min (Sepuri *et al.*, 2012). Sample buffer was added to the pellets, and the protein suspensions were resolved on an SDS–PAGE, the gel western transferred, and the membrane probed with the antibodies.

Ni pull-down assay

Soluble bacterial protein fraction enriched in recombinant Mxr2 and yeast mitochondrial fractions containing Flag-Mxr2 or Flag alone were solubilized in RIPA buffer. The fractions were precleared with Talon metal affinity resin and the supernatants collected. Purified recombinant His-Mge1 or His-Mge1 M155L (Marada *et al.*, 2013) proteins was treated with increasing concentrations of H_2O_2 for 2 h before allowing it to bind to Ni-NTA beads. The precleared Mxr2 containing bacterial lysate fractions or mitochondrial fraction containing Flag-Mxr2 was added to the Ni-NTA beads, which had been prebound with His-Mge1 in separate assays. The samples were kept on a rotisserie for 1 h at 4°C and washed three times in PBS/RIPA buffer containing 10 mM imidazole; the beads were collected by centrifuging at 2000 rpm for 5 min at 4°C. The beads were directly processed for SDS–PAGE, followed by Coomassie staining or Western immunoblotting.

Coimmunoprecipitation

A 500-µg amount mitochondria from yeast expressing Flag-Mxr2 was suspended in 100 µl of SEM buffer and centrifuged at 10,000 rpm for 10 min. The mitochondrial pellet was solubilized in RIPA buffer and precleared with protein A beads (GE Healthcare). The resultant supernatant was incubated with FLAG M2 (Sigma-Aldrich) antibody or control immunoglobulin G (IgG) at 4°C on a rotisserie for 4 h before addition of protein A beads. The sample was centrifuged at 2000 rpm and the beads washed three times with RIPA buffer. The beads were suspended in sample buffer without β-mercaptoethanol and loaded on an SDS–PAGE gel to resolve the bound proteins. The resolved proteins were Western transferred, and the membrane was probed with Flag and Mge1 antibodies.

Mxr2 enzymatic assay

The enzyme activity assay of Mxr2 was followed as described (Le *et al.*, 2009). The activity of oxidized protein (50 µM) or free MetO (1 mM) was assayed at 37°C in 50 mM sodium phosphate buffer, pH 7.2, containing 50 mM NaCl, 0.2 mM NADPH, 10 µg thioredoxin, and 20 µg thioredoxin reductase (Tarrago *et al.*, 2012). Recombinant His-Mge1 and GST proteins were treated with 20 mM H_2O_2 for 4 h and dialyzed overnight before addition to the assay. The assay was initiated with the addition of Mxr2, and the decrease in absorption at 340 nm was continuously monitored for 60 min. A small decrease in the absorption with Mxr2 control in the absence of substrate was deducted at all time points and used to calculate the enzymatic activity of Mxr2.

ATPase assay of mHsp70

ATPase activity assay was performed as described (Marada *et al.*, 2013) with minor modifications. Recombinant Mge1 was treated with 5 mM H_2O_2 for 2 h and incubated with or without 5 µg His-Mxr2 in presence of 10 mM DTT before using it for ATPase activity assay of Hsp70. An equivalent amount of His-Mxr2 was used in the control reactions, which had Hsp70 or Hsp70 and Mge1 before the start of the ATPase assay. The amount of radioactive P_i released at various time points was measured in a scintillation counter.

ROS measurement

Yeast strains were grown overnight in liquid medium before dilution in 10 ml of required medium at a starting OD_{600} of 0.1. The cultures were allowed to grow at 30°C until they reached OD_{600} of 1.0. Dichlorofluorescin diacetate (DCFDA), 20 µM, was added to the cultures and further incubated for 1 h at 30°C. Next the cells were washed and suspended in 100 µl of PBS. The intensity of fluorescence was measured in a fluorescence spectrophotometer (PerkinElmer, Waltham, MA) with an excitation wavelength of 480 nm and an emission wavelength of 525 nm; the emission was taken as the total ROS level.

Purification of His-Mge1 from yeast cells

For purification of His-Mge1, yNB134 and yNB135 strains were grown in 4 l of YPGE medium at 30°C until the cultures reached OD_{600} of 1. Cells were harvested by centrifuging the cultures at 5000 rpm. Cells were washed with double-distilled water and lysed with lyticase in 1.2 M sorbitol buffer. After formation of 50% spheroplasts, lysis buffer (6 M guanidium chloride, 150 mM NaCl, 50 mM Tris-HCl, pH 8.0, 10 mM imidazole, and 5 mM β-mercaptoethanol)

was added. Lysates were precleared by centrifuging the samples at 10,000 rpm for 10 min to remove cell debris. Ni-NTA beads were added to the lysates and incubated on a rotisserie for 4 h at room temperature. The Ni-NTA beads were collected by spinning the samples at 2000 rpm for 5 min. The beads were washed three times with wash buffer (6 M guanidium chloride, 150 mM NaCl, 50 mM Tris-HCl, pH 8.0, 20 mM imidazole, and 5 mM β-mercaptoethanol), followed by another wash with PBS buffer, pH 7.2. His-Mge1 protein was eluted in 400 mM imidazole in PBS buffer and resolved by SDS–PAGE. The gel was Coomassie stained, and the His-Mge1 protein band was excised and submitted for mass spectrometry analysis.

In vitro treatment of Mge1 with H_2O_2 and Mxr2 for MALDI-TOF analysis

Mge1 protein was oxidized with 20 mM H_2O_2 in PBS for 6 h and dialyzed in PBS, pH 7.2, overnight to remove H_2O_2. A 20-μg amount of Mge1 protein pretreated with H_2O_2 was incubated with or without Mxr2 (2.5 μg) protein in presence of 10 mM DTT in 50 mM NaCl and 50 mM sodium phosphate buffer, pH 7.2. After 4 h of incubation at room temperature, samples were processed for SDS–PAGE, and the gel was Coomassie stained. The Mge1 protein bands were excised and sent for mass spectrophotometric analysis at the proteomics facilities at the University of Hyderabad (Hyderabad, India) and the Indian Institute of Sciences (Bangalore, India).

Mass spectrometry

For mass spectrometric analysis, all protein samples were separated by SDS–PAGE and Coomassie stained, and the protein band was excised and subjected to mass spectrometry analysis. Proteins were reduced (10 mM DTT) and alkylated (10 mM iodoacetamide) using standard protocols, followed by in-gel trypsin/LysC overnight digestion at 37°C. Peptides were concentrated in a vacuum centrifuge at room temperature and suspended in 0.1% trifluoroacetic acid/25% acetonitrile. The peptides were analyzed by MALDI-TOF/MS and MALDI-TOF/TOF/MS/MS. MALDI spectra were obtained using a Bruker Daltonics mass spectrometer. Peptide Mass Fingerprint search was performed using the MASCOT server for protein identification. Graphs were plotted by taking percentage of relative intensity in relation to the peptide of interest. MS/MS fragment ions were assigned by comparing with predicted ions generated in silico by using a Protein Prospector (University of California, San Francisco, CA).

Protein aggregation assay

For each protein aggregation assay, 50 μg of mitochondria was suspended in aggregation assay buffer (250 mM sucrose, 10 mM MOPS, 80 mM KCl, 5 mM $MgCl_2$, 5 mM ATP, and 4 mM NADH) and treated with H_2O_2 for 30 min at room temperature (Bender *et al.*, 2011). The mitochondria were centrifuged at 10,000 rpm for 10 min, and the pellet was solubilized in lysis buffer (0.5% Triton X-100, 200 mM KCl, 30 mM Tris-HCl, pH 7.5, 5 mM EDTA). The solubilized mitochondria were centrifuged at 25,000 rpm for 1 h. The supernatant fraction (soluble fraction) was collected, and the pellet (aggregated fraction) was resuspended in lysis buffer. Twenty percent of supernatant fraction and total pellet fraction was separated by SDS–PAGE, and the gel was silver stained.

ACKNOWLEDGMENTS

This work was supported by grants from the Council of Scientific and Industrial Research, Department of Science and Technology, India, to N.B.V.S. and a Department of Science and Technology Fund for Improvement of S&T Infrastructure grant to the Department of Biochemistry, University of Hyderabad. We acknowledge a Department of Science and Technology Promotion of University Research and Scientific Excellence grant to the University of Hyderabad. We thank D. Pain, University of Medicine and Dentistry of New Jersey (Newark, NJ), for sharing the mHsp70 antibody; Krishnaveni Mishra for providing MXR deletion strains; and Charles Williams for providing Trx and TrxR plasmids. We thank T.E. Dever (National Institutes of Health, Bethesda, MD) for providing Fun12 antibody. We acknowledge the following for providing fellowships: the Council of Scientific and Industrial Research (A.P.K. and K.S.), the University Grants Commission–Basic Scientific Research (A.M.), and the Indian Council of Medical Research (Y.B.). We thank Monica Kannan and Raghu Tadala for carrying out proteomic studies and all the members of N.B.V.S.'s laboratory for comments and suggestions.

REFERENCES

Beinert H, Holm RH, Münck E (1997). Iron-sulfur clusters: nature's modular, multipurpose structures. Science 277, 653–659.

Bender T, Lewrenz I, Franken S, Baitzel C, Voos W (2011). Mitochondrial enzymes are protected from stress-induced aggregation by mitochondrial chaperones and the Pim1/LON protease. Mol Biol Cell 22, 541–554.

Boschi-Muller S, Gand A, Branlant G (2008). The methionine sulfoxide reductases: Catalysis and substrate specificities. Arch Biochem Biophys 474, 266–273.

Chacinska A, Koehler CM, Milenkovic D, Lithgow T, Pfanner N (2009). Importing mitochondrial proteins: machineries and mechanisms. Cell 138, 628–644.

Ciorba MA, Heinemann SH, Weissbach H, Brot N, Hoshi T (1997). Modulation of potassium channel function by methionine oxidation and reduction. Proc Natl Acad Sci USA 94, 9932–9937.

De Los Rios P, Goloubinoff P (2012). Protein folding: chaperoning protein evolution. Nat Chem Biol 8, 226–228.

D'Silva P, Liu Q, Walter W, Craig EA (2004). Regulated interactions of mtHsp70 with Tim44 at the translocon in the mitochondrial inner membrane. Nat Struct Mol Biol 11, 1084–1091.

Erickson JR, Joiner ML, Guan X, Kutschke W, Yang J, Oddis CV, Bartlett RK, Lowe JS, O'Donnell SE, Aykin-Burns N, *et al.* (2008). A dynamic pathway for calcium-independent activation of CaMKII by methionine oxidation. Cell 133, 462–474.

Finkel T, Holbrook NJ (2000). Oxidants, oxidative stress and the biology of ageing. Nature 408, 239–247.

Gabbita SP, Aksenov MY, Lovell MA, Markesbery WR (1999). Decrease in peptide methionine sulfoxide reductase in Alzheimer's disease brain. J Neurochem 73, 1660–1666.

Gietz RD, Woods RA (2002). Transformation of yeast by lithium acetate/single-stranded carrier DNA/polyethylene glycol method. Methods Enzymol 350, 87–96.

Glaser CB, Yamin G, Uversky VN, Fink AL (2005). Methionine oxidation, alpha-synuclein and Parkinson's disease. Biochim Biophys Acta 1703, 157–169.

Grimshaw JP, Jelesarov I, Schönfeld HJ, Christen P (2001). Reversible thermal transition in GrpE, the nucleotide exchange factor of the DnaK heat-shock system. J Biol Chem 276, 6098–6104.

Harrison CJ, Hayer-Hartl M, Di Liberto M, Hartl F, Kuriyan J (1997). Crystal structure of the nucleotide exchange factor GrpE bound to the ATPase domain of the molecular chaperone DnaK. Science 276, 431–435.

Hartl FU, Bracher A, Hayer-Hartl M (2011). Molecular chaperones in protein folding and proteostasis. Nature 475, 324–332.

Hung R-J, Spaeth CS, Yesilyurt HG, Terman JR (2013). SelR reverses Mical-mediated oxidation of actin to regulate F-actin dynamics. Nat Cell Biol 15, 1445–1454.

Iosefson O, Sharon S, Goloubinoff P, Azem A (2012). Reactivation of protein aggregates by mortalin and Tid1–the human mitochondrial Hsp70 chaperone system. Cell Stress Chaperones 17, 57–66.

Kantorow M, Hawse JR, Cowell TL, Benhamed S, Pizarro GO, Reddy VN, Hejtmancik JF (2004). Methionine sulfoxide reductase A is important for lens cell viability and resistance to oxidative stress. Proc Natl Acad Sci USA 101, 9654–9659.

Kaya A, Koc A, Lee BC, Fomenko DE, Rederstorff M, Krol A, Lescure A, Gladyshev VN (2010). Compartmentalization and regulation of mitochondrial function by methionine sulfoxide reductases in yeast. Biochemistry 49, 8618–8625.

Kim H-Y, Gladyshev VN (2004). Methionine sulfoxide reduction in mammals: characterization of methionine-R-sulfoxide reductases. Mol Biol Cell 15, 1055–1064.
Knight SA, Sepuri NB, Pain D, Dancis A (1998). Mt-Hsp70 homolog, Ssc2p, required for maturation of yeast frataxin and mitochondrial iron homeostasis. J Biol Chem 273, 18389–18393.
Laloraya S, Dekker PJ, Voos W, Craig EA, Pfanner N (1995). Mitochondrial GrpE modulates the function of matrix Hsp70 in translocation and maturation of preproteins. Mol Cell Biol 15, 7098–7105.
Langer T, Lu C, Echols H, Flanagan J, Hayer MK, Hartl FU (1992). Successive action of DnaK, DnaJ and GroEL along the pathway of chaperone-mediated protein folding. Nature 356, 683–689.
Le DT, Lee BC, Marino SM, Zhang Y, Fomenko DE, Kaya A, Hacioglu E, Kwak GH, Koc A, Kim HY, Gladyshev VN (2009). Functional analysis of free methionine-R-sulfoxide reductase from Saccharomyces cerevisiae. J Biol Chem 284, 4354–4364.
Lennon BW, Williams CH (1995). Effect of pyridine nucleotide on the oxidative half-reaction of Escherichia coli thioredoxin reductase. Biochemistry 34, 3670–3677.
Levine RL, Moskovitz J, Stadtman ER (2000). Oxidation of methionine in proteins: roles in antioxidant defense and cellular regulation. IUBMB Life 50, 301–307.
Lutz T, Westermann B, Neupert W, Herrmann JM (2001). The mitochondrial proteins Ssq1 and Jac1 are required for the assembly of iron sulfur clusters in mitochondria. J Mol Biol 307, 815–825.
Marada A, Allu PK, Murari A, PullaReddy B, Tammineni P, Thiriveedi VR, Danduprolu J, Sepuri NBV (2013). Mge1, a nucleotide exchange factor of Hsp70, acts as an oxidative sensor to regulate mitochondrial Hsp70 function. Mol Biol Cell 24, 692–703.
Mayer MP, Bukau B (2005). Hsp70 chaperones: cellular functions and molecular mechanism. Cell Mol Life Sci 62, 670–684.
Mehl AF, Heskett LD, Jain SS, Demeler B (2003). Insights into dimerization and four-helix bundle formation found by dissection of the dimer interface of the GrpE protein from Escherichia coli. Protein Sci 12, 1205–1215.
Meyer Y, Buchanan BB, Vignols F, Reichheld J-P (2009). Thioredoxins and glutaredoxins: unifying elements in redox biology. Annu Rev Genet 43, 335–367.
Midwinter RG, Cheah F-C, Moskovitz J, Vissers MC, Winterbourn CC (2006). IκB is a sensitive target for oxidation by cell-permeable chloramines: inhibition of NF-κB activity by glycine chloramine through methionine oxidation. Biochem J 396, 71–78.
Moskovitz J (2005). Methionine sulfoxide reductases: ubiquitous enzymes involved in antioxidant defense, protein regulation, and prevention of aging-associated diseases. Biochim Biophys Acta 1703, 213–219.
Murphy MP (2009). How mitochondria produce reactive oxygen species. Biochem J 417, 1–13.
Orrenius S, Gogvadze V, Zhivotovsky B (2007). Mitochondrial oxidative stress: implications for cell death. Annu Rev Pharmacol Toxicol 47, 143–183.
Packschies L, Theyssen H, Buchberger A, Bukau B, Goody RS, Reinstein J (1997). GrpE accelerates nucleotide exchange of the molecular chaperone DnaK with an associative displacement mechanism. Biochemistry 36, 3417–3422.
Pamplona R, Costantini D (2011). Molecular and structural antioxidant defenses against oxidative stress in animals. Am J Physiol Regul Integr Comp Physiol 301, R843–R863.
Savel'ev AS, Novikova LA, Kovaleva IE, Luzikov VN, Neupert W, Langer T (1998). ATP-dependent proteolysis in mitochondria. m-AAA protease and PIM1 protease exert overlapping substrate specificities and cooperate with the mtHsp70 system. J Biol Chem 273, 20596–20602.
Sepuri NBV, Gorla M, King MP (2012). Mitochondrial lysyl-tRNA synthetase independent import of tRNA lysine into yeast mitochondria. PLoS One 7, e35321.
Styskal J, Nwagwu FA, Watkins YN, Liang H, Richardson A, Musi N, Salmon AB (2013). Methionine sulfoxide reductase A affects insulin resistance by protecting insulin receptor function. Free Radic Biol Med 56, 123–132.
Tammineni P, Anugula C, Mohammed F, Anjaneyulu M, Larner AC, Sepuri NBV (2013). The import of the transcription factor STAT3 into mitochondria depends on GRIM-19, a component of the electron transport chain. J Biol Chem 288, 4723–4732.
Tarrago L, Kaya A, Weerapana E, Marino SM, Gladyshev VN (2012). Methionine sulfoxide reductases preferentially reduce unfolded oxidized proteins and protect cells from oxidative protein unfolding. J Biol Chem 287, 24448–24459.
Uzarska MA, Dutkiewicz R, Freibert S-A, Lill R, Mühlenhoff U (2013). The mitochondrial Hsp70 chaperone Ssq1 facilitates Fe/S cluster transfer from Isu1 to Grx5 by complex formation. Mol Biol Cell 24, 1830–1841.
Westermann B, Prip-Buus C, Neupert W, Schwarz E (1995). The role of the GrpE homologue, Mge1p, in mediating protein import and protein folding in mitochondria. EMBO J 14, 3452–3460.
Winterbourn CC, Hampton MB (2008). Thiol chemistry and specificity in redox signaling. Free Radic Biol Med 45, 549–561.
Wright G, Terada K, Yano M, Sergeev I, Mori M (2001). Oxidative stress inhibits the mitochondrial import of preproteins and leads to their degradation. Exp Cell Res 263, 107–117.
Wu B, Ang D, Snavely M, Georgopoulos C (1994). Isolation and characterization of point mutations in the Escherichia coli grpE heat shock gene. J Bacteriol 176, 6965–6973.
Zhang X-H, Weissbach H (2008). Origin and evolution of the protein-repairing enzymes methionine sulphoxide reductases. Biol Rev Camb Philos Soc 83, 249–257.